Competition between fermions and bosons in nuclear matter at low densities and finite temperatures

J. Mabiala, H. Zheng, A. Bonasera, Z. Kohley, and S. J. Yennello

Phys. Rev. C **94**, 064617 — Published 29 December 2016

DOI: 10.1103/PhysRevC.94.064617

Competition between fermions and bosons in nuclear matter at low densities and finite temperatures

J. Mabiala,[1,*] H. Zheng,[2] A. Bonasera,[2,3] Z. Kohley,[4] and S. J. Yennello[3,5]

[1] *INFN, Laboratori Nazionali di Legnaro, Italy*
[2] *Laboratori Nazionali del Sud, INFN, via Santa Sofia, 62, 95123 Catania, Italy*
[3] *Cyclotron Institute, Texas A&M University, College Station, Texas 77843, USA*
[4] *National Superconducting Cyclotron Laboratory, Michigan State University, East Lansing, Michigan 48824, USA*
[5] *Chemistry Department, Texas A&M University, College Station, Texas 77843, USA*

(Dated: December 11, 2016)

We derive the free energy for fermions and bosons from fragmentation data. Inspired by the symmetry and pairing energy of the Weizsäcker mass formula we obtain the free energy of fermions (nucleons) and bosons (alphas and deuterons) using Landau's free energy approach. We confirm previously obtained results for fermions and show that the free energy for alpha particles is negative and close to the free energy for ideal Bose gases and in perfect agreement with the free energy of an interacting Bose gas under the repulsive Coulomb force. Deuterons behave more similarly to fermions (positive free energy) rather than bosons, which is probably due to their low binding energy. We show that the α-particle fraction is dominant at all temperatures and densities explored in this work. This is consistent with their negative free energy, which favors clusterization of nuclear matter into α-particles at subsaturation densities and finite temperatures.

PACS numbers: 25.70.–z, 21.65.–f, 25.70.Mn, 42.50.Lc

I. INTRODUCTION

Dilute mixed systems composed of fermions and bosons exhibit a large variety of interesting features that have been the subject of several theoretical and experimental works. Although generally considered as made of strongly interacting fermions (protons and neutrons), nucleonic systems have been observed to display some properties relevant of bosons. Some of these aspects are the α-decay in heavy nuclei, preformed α-particles in the ground state of nuclei [1] and the cluster structure of N=Z=even light nuclei [2]. While the tunneling through the Coulomb barrier is well understood, the preformation of the α-particle is still a difficult task for theoretical model descriptions. Recently, *ab initio* lattice simulations have shown that, depending on the form of the interaction between nucleons, the ground states of certain light nuclei lie near a quantum phase transition between a Bose-condensed gas of alpha particles and a nuclear liquid [3, 4].

Experiments in heavy-ion reactions at energies around the Fermi energy have revealed the creation of dilute nuclear matter in which the strong interaction has led to the emergence of correlated states of nucleons (clusters). These few-body correlations remain substantial even at very small densities ($\backsim 0.01\rho_0$ or less; ρ_0=0.15 nucl/fm^3) and at moderate temperatures [5–9]. In fact, at low densities the system can minimize its energy by forming light clusters such as deuterons or strongly bound α-particles. Clustering effects are expected to modify the density dependence of the symmetry energy of nuclear matter [10, 11], and the structure of atomic nuclei [2].

The thermodynamic properties of nuclear matter play an important role in studies of various astrophysical phenomena [12–15]. Knowledge of thermodynamic quantities such as the free energy of fragments is needed when considering a wide range of temperatures, densities and/or proton fractions. In fact, the free energy of fragments defines the balance between denser fragments and the more dilute nucleonic gas. Its changes with temperatures and densities are of crucial importance to better understand the properties of dense nuclear matter.

In this paper, we report on experimental free energy (density) for fermions and bosons from the fragmentation of quasiprojectiles by application of Landau's free-energy approach. The temperature and density of the produced quasiprojectile systems are determined using the quantum-fluctuation method, fully described in Refs. [16–20]. We notice, and it is an important result, that the free-energy density for alphas is negative. In contrast, it is positive for deuterons, and close to that for fermions. The free-energy density for ideal Bose gases gives results similar to those for alphas but has opposite sign for those of deuterons. This demonstrates that alphas behave indeed as bosons while deuterons do not and are suppressed, probably due to their low binding energy. The fact that the free-energy density is negative means that if N=Z=even systems will 'live' long enough, all the particles will cluster into alphas while deuterons will disappear.

II. EXPERIMENT, EVENT SELECTION AND RECONSTRUCTION

The experiment was performed at the Cyclotron Institute, Texas A&M University. Beams at 35 MeV/A of

* E-mail address: justin.mabiala@lnl.infn.it

^{64}Zn, ^{70}Zn, and ^{64}Ni from the K-500 superconducting cyclotron were used to respectively irradiate self supporting targets of ^{64}Zn, ^{70}Zn, and ^{64}Ni. The 4π NIMROD-ISiS setup [21, 22] was used to collect charged particles and free neutrons produced in the reactions. A detailed description of the experiment can be found in Refs. [23–25]. For events in which all charged particles were isotopically identified, the quasiprojectile (QP) was reconstructed using the charged particles and free neutrons. This reconstruction includes, therefore, determination of the QP composition, both A and Z. The neutron ball provided event-by-event experimental information on the free neutrons emitted during a reaction [26, 27]. Particles with Z=1, 2 and $Z \geq$3, detected by NIMROD-ISiS setup were attributed to QP decay when their longitudinal velocities lay within the range of ±65%, ±60%, ±40%, respectively, of the coincident QP residue velocity in the event [26, 28]. Thermally equilibrated QP events were selected by requiring the QP to be on average spherical, in a narrow range of shape deformation. The sum of the masses of the collected and accepted fragments was constrained to be in the range of $54 \leq A_{QP} \leq 64$. Events were then sorted in 8 QP excitation energy bins, 1 MeV/A wide, ranging from 2.5 to 9.5 MeV/A.

III. METHOD, RESULTS AND DISCUSSION

Recently, we have analyzed fragment yield data to investigate the nuclear phase transition using the Landau free energy technique [29–32]. This approach is based on the assumption that, in the vicinity of the critical point, the fragment free energy per nucleon (F_A) relative to the system temperature (T) can be expanded in a power series in the fragment's neutron-proton asymmetry m as

$$\frac{F_A}{T} = \frac{1}{2}am^2 + \frac{1}{4}bm^4 + \frac{1}{6}cm^6 - \frac{H}{T}m \ , \qquad (1)$$

where m=$(N - Z)/A$, and N, Z, and A are the neutron, proton, and mass numbers of the fragment, respectively. The quantity m behaves as an order parameter, H is its conjugate variable and the coefficients a, b, and c are fitting parameters. Notice that the inclusion of higher order terms have been deemed necessary in statistical models due to the formation of clusters in low density nuclear matter (see Eqs. 79, 80 and the following discussion in Ref. [33]). According to the modified Fisher model [29, 34, 35], the fragment yield is given by Y=$y_0 A_f^{-\tau} e^{-(F_A/T)A}$ near the critical point; with τ=2.3 ± 0.1 the critical exponent [29, 36] and y_0 a constant.

Figure 1(a) shows the fragment free energy (F_A/T) values as a function of their neutron-proton asymmetry m at an excitation energy of 5.5 MeV/A of the QP. One clearly sees that F_A/T values for N=Z fragments (m=0) significantly deviate from the regular behavior of the $N \neq Z$ fragments. This shows the significant role of odd-even

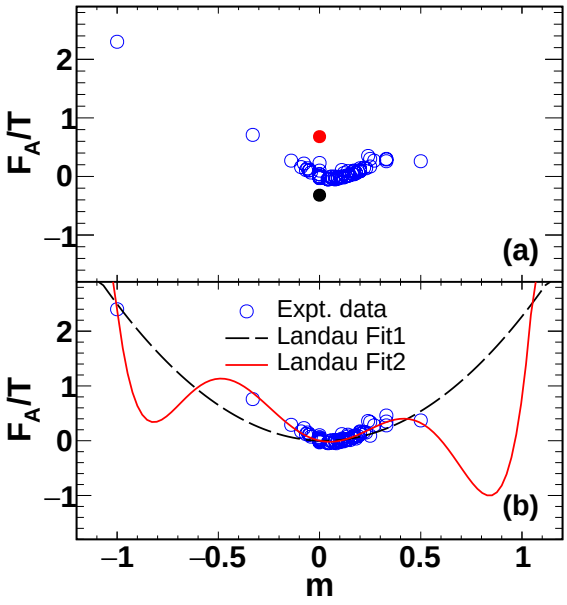

FIG. 1. (Color online) F_A/T for fragments as a function of fragment's neutron-proton asymmetry m for an excitation energy of 5.5 MeV/A of the QP. (a) F_A/T values calculated from fragment yield data normalized to the yield of ^{12}C. Data points corresponding to deuteron and α are colored in red and black, respectively. (b) F_A/T values calculated after correcting for pairing effects using a_p/T values obtained from the analysis of N=Z nuclei [29–32]. The dashed line (Landau Fit1) is a fit to data using only the first and last terms of Eq. (1). The solid line (Landau Fit2) represents a fit to data using the complete Landau free energy [Eq. (1)] with a, b, H/T as free parameters, and fixing c = 115 that was observed to be almost constant, within uncertainties, over the entire range of the QP excitation energy [32]. The values of a, b, and H/T corresponding to the solid line were obtained as 16.289±0.024, -102.871±0.058 and 0.808±0.002, respectively. Error bars corresponding to statistical errors are smaller than the symbols.

effects, which we will loosely refer to as pairing. We can generalize the Landau approach to include the free energy for m=0 particles, i.e., bosons. Inspired by the pairing energy per particle for a fragment with mass number A (E_p=$a_p\delta/A^{3/2}$), one obtains the following linear equation for the analysis of N=Z fragments

$$\ln(YA^{\tau}) = \ln(y_0) + \frac{a_p}{T}\frac{\delta}{A^{1/2}} \ , \qquad (2)$$

where a_p/T is the slope and $\ln(y_0)$ the intercept, and it is discussed in more details in Refs. [31, 32, 37]. The quantity δ=-1, 0 and +1 for odd-odd, odd-even and even-even fragments, respectively; the term Π=$\delta/A^{3/2}$ to be the order parameter in Landau's description and plays the same role as the order parameter m for the free energy. Higher order terms in Π might be possible but a good fit is obtained at this lowest order with the available data. A linear fit to the N=Z data allows the extraction of the values of a_p/T and y_0 [32].

In Fig. 1(b), F_A/T values corrected by "pairing" are shown. The dashed line (Landau Fit1) represents a fit to data using only the first and last terms of Eq. (1), a case corresponding to a single phase as in the Weizsäcker mass formula. The solid line (Landau Fit2) is a fit to data using the complete Landau free energy as given by Eq. (1). As the efficiency for measuring neutrons differs from the efficiency for measuring charged particles, neutron yields were excluded from the fitting. It is observed in the figure that the complete form of Eq. (1) provides a better fit to the free energy data. The appearance of the three minima is a signature of a first-order phase transition of the system [29–32, 38]. Of course no data points are present in the region of the minima thus the constraint is poor. We notice that nuclei having such values of the order parameter m are very exotic (for instance ^{10}He) and will decay quickly before reaching the detector.

The temperatures and densities of the QP are determined from the fluctuations of the transverse momentum quadrupole Q_{xy}=$p_x^2 - p_y^2$, average multiplicities and multiplicity fluctuations. These observables are used to correct for Coulomb effects as well. Further details can be found in Refs. [16–20]. We have applied the method of correcting for Coulomb effects to experimental data in Ref. [40], and it was observed that the Coulomb corrections lower temperature values by almost 2 MeV, but the effects on the densities were observed to be small. A similar procedure was also applied to the data from INDRA-collaboration for p, d and α [41] and their results are consistent with ours. In Ref. [42], the error in applying the Coulomb corrections which arises from the uncertainty in the source charge was estimated to be respectively ±2% for the densities and ±6% for the temperatures.

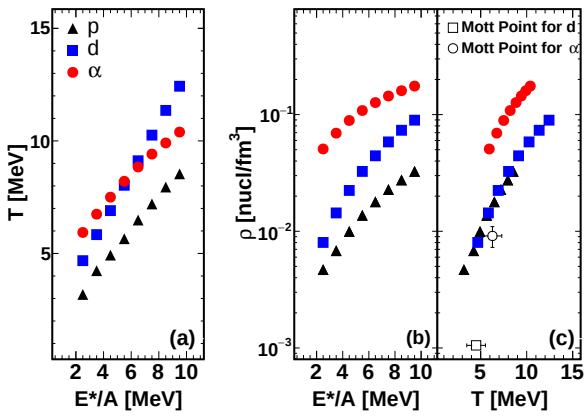

FIG. 2. (Color online) (a) and (b) Temperatures and densities sampled by three probe light particles (p, d and α) emitted by the QP as a function of its excitation energy. (c) Density plotted as a function of temperature for p, d and α. Error bars corresponding to statistical errors are smaller than the symbols. For comparison, experimentally derived Mott points for d (empty square) and α (empty circle) are also shown [39].

The QP temperatures (T) and densities (ρ) sampled by protons (p), deuterons (d) and alphas (α) as a function of the excitation energy per nucleon of the reconstructed QP, E^*/A, are shown in Fig. 2(a) and Fig. 2(b). Since the evaluation of associated errors on T and ρ was not straightforward, we have estimated the physical values from the difference in extracted values between the full and half datasets. Estimated statistical errors on T and ρ are smaller than the symbols (better than 3%). These errors do not, however, include the uncertainty from Coulomb corrections. T and ρ values for the three light particles are observed to rise with E^*/A. While T values for d and α are very close, the densities seen by the two particles are very different from each other. We also observe that densities probed by alphas are slightly higher than ρ_0 at highest E^*/A values, which we will discuss further later. We have to stress that densities and temperatures of bosons are derived under the assumption of Coulomb repulsion among fragments. Of course at higher densities these fragments will start to overlap and the attractive nuclear force might become dominant. Boson systems below the critical point (condensate) become unstable if an attractive force is at play [38], thus we expect our approximation to break down at some density and temperature. Since the temperature for which near ground-state densities are reached is rather high, the kinetic energy might be dominant with respect to the interactions and our approximation should still be valid. In fact, very recent *ab initio* nuclear structure calculations have shown that for particular interactions the nuclear ground state undergoes a quantum phase transition from BEC to a nuclear liquid [3, 4].

The correlation between the density and the temperature, as probed by p, d and α, is presented in Fig. 2(c). It is interesting to see that p and d display one single curve, even though there is a clear difference for the behavior of their sampled T and ρ with E^*/A. The binding energy of a cluster relative to the medium vanishes at a point known as the Mott point[33]. Since we observe alphas coming from high densities, we have shown the Mott points for d and α obtained in Ref. [39] for comparison. Note that the method to derive the Mott point [39] is based on classical approximations at variance with our quantum approach and we have used a different way to correct for Coulomb effects [40]. It is also useful to stress that fragments can still be formed above the Mott point due to quantum fluctuations [11].

After deriving T values, we apply Eq. (1), using the extracted Landau's fitting parameters, to determine the fragment free energy per nucleon, F_A, for fermions. For bosons (d and α), we adopt the parametrization F_A=$-a_p\delta/A^{3/2}$ to easily derive the free energy. Figures 3(a)-(b) depict the temperature and density dependence of the derived values of F_A for p, d and α. Estimated statistical errors on F_A for protons are 10% while those for d and α are smaller than the symbols (better than 3%). There is a strong correlation of increasing F_A with increasing T and ρ, for p and d. In contrast to p and d

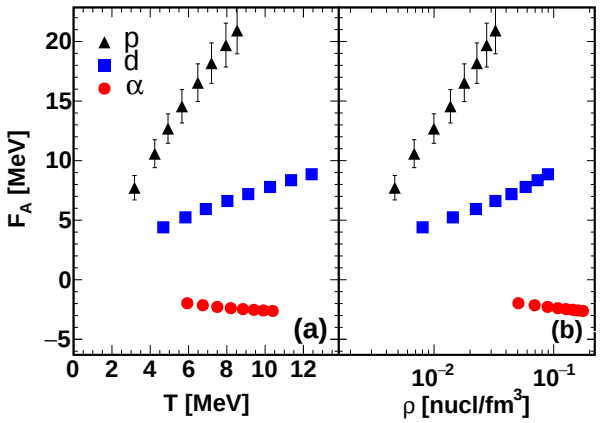

FIG. 3. (Color online) Free energy for p, d and α calculated within the framework of Landau's approach as a function of their sampled temperature (a) and density (b). Error bars are shown when statistical errors exceed the size of the symbols.

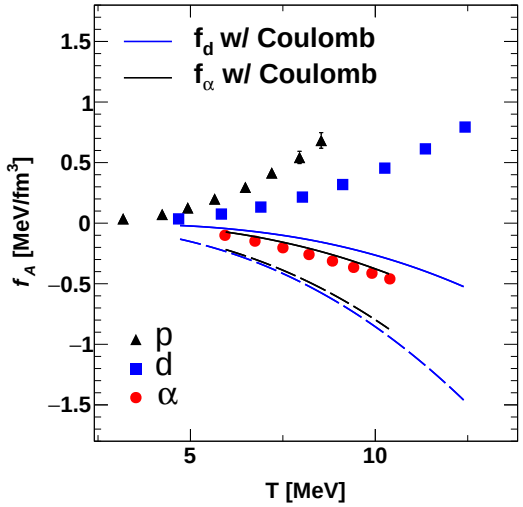

FIG. 4. (Color online) Free-energy density (f_A=$F_A \times \rho$) as a function of temperature for the three light particles. Error bars are shown when statistical errors exceed the size of the symbols. Solid lines refer to the Coulomb corrected free-energy density for d and α – Eq. (A.11) in the Appendix. The dashed lines are the corresponding ideal Bose gas limit [43], Eq. (3).

results, F_A values for α are negative and weakly depend on T and ρ. From the values of F_A and ρ, we examine in Fig. 4 the free energy density (f_A=$F_A \times \rho$) against T. It is observed that f_A approaches zero in the limit $T \to 0$ MeV, as expected, and differences between p and d curves seen in Fig. 3(a)-(b) are less pronounced. In Fig. 4, both the f_A results obtained for an ideal Bose

TABLE I. Densities, temperatures, free energies and mass fractions for p, d and α.

		p		
E^*/A [MeV]	ρ [nucl/fm^3]	T [MeV]	F_A [MeV]	X_p
2.5	0.0047	3.2	7.73	0.016
3.5	0.0068	4.2	10.58	0.020
4.5	0.0100	4.9	12.69	0.024
5.5	0.0137	5.7	14.56	0.029
6.5	0.0179	6.5	16.54	0.034
7.5	0.0228	7.2	18.18	0.039
8.5	0.0275	7.9	19.70	0.044
9.5	0.0326	8.5	20.93	0.049
		d		
E^*/A [MeV]	ρ [nucl/fm^3]	T [MeV]	F_A [MeV]	X_d
2.5	0.0080	4.7	4.401	0.012
3.5	0.0144	5.8	5.237	0.018
4.5	0.0224	6.9	5.936	0.024
5.5	0.0326	8.0	6.610	0.030
6.5	0.0443	9.1	7.190	0.036
7.5	0.0583	10.3	7.790	0.043
8.5	0.0734	11.3	8.357	0.049
9.5	0.0896	12.4	8.856	0.055
		α		
E^*/A [MeV]	ρ [nucl/fm^3]	T [MeV]	F_A [MeV]	X_α
2.5	0.0507	5.9	-1.973	0.114
3.5	0.0693	6.7	-2.140	0.143
4.5	0.0890	7.5	-2.280	0.171
5.5	0.1084	8.2	-2.389	0.193
6.5	0.1268	8.8	-2.465	0.210
7.5	0.1443	9.4	-2.528	0.225
8.5	0.1603	9.9	-2.578	0.237
9.5	0.1756	10.4	-2.618	0.245

gas (dashed lines) and for a Coulomb corrected Bose gas (solid lines) are shown. Recall that the free energy density for an ideal Bose gas is given by:

$$f_A = -0.085 g_A \frac{m_A^{3/2} T^{5/2}}{\hbar^3} \ , \qquad (3)$$

where g_A is the degeneracy factor, T refers to the temperature sampled by the fragment species A and m_A its mass. When Coulomb correction is taken into account, Eq. (3) is modified as given in the Appendix and can be solved numerically. Eq. (3) displays no density dependence of the free energy density which is an unphysical result [43]. This well-known negative feature of the ideal Bose gas [38] is easily corrected if there is a repulsive interaction among the Bosons. In fact when implementing the Coulomb correction in the free-energy density calculation, Appendix, the result is in very good agreement to the experiment, Fig. 4. The good agreement between the calculation and the experimental results is quite in-

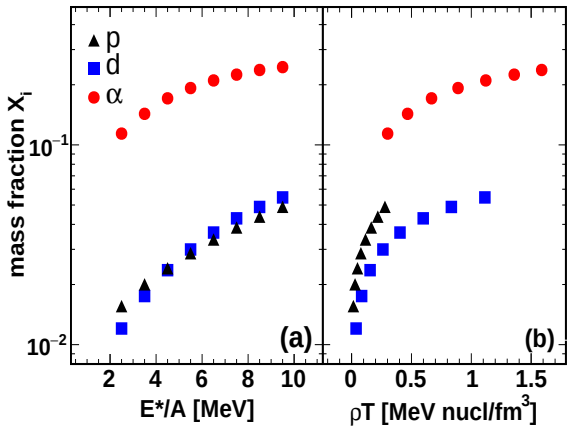

FIG. 5. (Color online) Mass fractions of p, d and α are shown as a function of E^*/A (a) and of the 'kinetic pressure' $\rho \times T$ (b). Statistical errors are smaller than the symbols.

teresting since they have been obtained in completely different manners, one from the experimental yield distribution and the other from the Coulomb corrected free energy density for Bosons. The ideal gas limit displays a similar behavior of the data but slightly shifted downwards. Notice also the different theoretical behavior of d and α with and without Coulomb corrections. The positive experimentally-derived f_A values for d indicate that these particles behave much like fermions, probably because of their low binding energy. For a system in equilibrium, this implies that the system of nucleons will predominantly coalesce into α-particles.

In theoretical models cluster mass fractions are commonly used to characterize the degree of clusterization in low-density matter. Figure 5(a) shows mass fractions, X_i=n_iA_i/A_{QP}, of the three light particles as a function of E^*/A, derived directly from data. The quantities n_i and A_i are, respectively, the multiplicity and mass of particle i, and A_{QP} denotes the mass of the reconstructed fragmenting source (A_{QP} ≈60). While a higher α-cluster fraction is seen for all E^*/A values, p and d have similar mass fractions. In Fig. 5(b), the behavior of X_i is displayed as a function of the 'kinetic pressure' $\rho \times T$. In Ref. [33], in which a microscopic quantum statistical approach and a generalized relativistic mean-field model were employed, it was reported that complex particles may still appear beyond the Mott point, and X_α was found to decrease at high ρ. However, our results show that X_α is enhanced at high E^*/A and, correspondingly, at high T and ρ. An increase of the α-particle fraction with density (and temperature) very similar to our findings has been observed in calculations of symmetric nuclear matter using the virial expansion [10]. A less marked increase with mass fraction values below the one reported in Fig. 5 has been found in the nuclear statistical equilibrium model [33]. Other models such as the EOS of Shen *et al.* [44], the relativistic mean field model and quantum statistical approaches [33, 45] display a rather sharp dissolution of alpha particles with densities above some 10^{-2} fm^{-3}. Such a sharp dissolution is due to Pauli blocking [33] or excluded volume effects [44, 45]. For reference, compare Fig. 15 in Ref. [33] and Fig. 13 in Ref. [45] to Fig. 5. Some of these models predict also the survival of d at higher densities than α-particles. This feature has never been reported in the literature of multifragmentation data to our knowledge, including this work– Fig. 5, where α-particles are very abundantly produced at variance with deuterons. As we have stressed before, the assumption of only a repulsive Coulomb interaction is valid at low densities. For increasing densities the nuclear attraction makes the BEC [3] unstable. However, in our case we obtain densities (especially for α-particles) near the ground state densities for temperatures higher than 5 MeV. For such temperatures the (attractive) nuclear interactions become negligible; thus our approximations could remain valid. However, it is necessary to investigate this point further in order to asses the role of nuclear interactions in the determination of the density (near and above the ground state) and the temperature. The high-density results reported in this work, even though in reasonable agreement with the free (and the Coulomb corrected) Bose gas limit, Fig. 3, should be taken *cum grano salis*. Our results are summarized in Table I which includes all quantities discussed here.

IV. SUMMARY

In summary, we have extracted the free energy (density) for fermions and bosons in finite nuclei at subsaturation densities and finite temperatures using the Landau free energy technique. It was found that free-energy results for α-particles are negative and close to those of ideal (and Coulomb corrected) Bose gases, whereas deuterons behave much like fermions. The α-particle fraction was shown to be favored at all temperatures and densities explored in this work. The present results are consistent with the clusterization of nuclear matter into α-particles. In the limit of zero temperature and ground-state density, the free energy discussed above reduces to the symmetry and pairing terms in the Weizsäcker mass formula.

Appendix

Let us assume particles follow the Bose-Einstein distribution modified by the Coulomb correction,

$$f(p) = \frac{1}{e^{[\frac{p^2}{2m} + \frac{1.44\times 4\pi\hbar^2 q_1 q_2}{V p^2} - \mu]/T} - 1}, \qquad (A.1)$$

where μ is the chemical potential and T is the temperature, V the volume, q_1 and q_2 the particle and source charges respectively. The free energy of a Bose gas is

$$F = E - TS = N\mu - PV, \tag{A.2}$$

which can be easily transformed as

$$\begin{aligned}\frac{F}{V} &= \frac{N}{V}\mu - P \\ &= \rho\mu - P.\end{aligned} \tag{A.3}$$

Therefore, we need to calculate the pressure P for a Bose gas with Coulomb correction. From Ref. [46] [section 6.4 (for boson case)], the pressure P can be obtained as

$$\begin{aligned}P &= \frac{gT}{-1}\int_0^\infty \ln[1 - ze^{-\beta\varepsilon(p)}]\frac{4\pi p^2}{h^3}dp \\ &= -\frac{4\pi gT}{h^3}\left\{\frac{p^3}{3}\ln[1 - ze^{-\beta\varepsilon(p)}]\Big|_0^\infty \right. \\ &\quad \left. - \int_0^\infty \frac{p^3}{3}\frac{-ze^{-\beta\varepsilon(p)}}{1 - ze^{-\beta\varepsilon(p)}}(-\beta)\frac{\partial\varepsilon(p)}{\partial p}dp\right\} \\ &= \frac{4\pi g}{3h^3}\int_0^\infty \frac{ze^{-\beta\varepsilon(p)}}{1 - ze^{-\beta\varepsilon(p)}}p^3\frac{\partial\varepsilon(p)}{\partial p}dp \\ &= \frac{4\pi g}{3h^3}\int_0^\infty \frac{1}{z^{-1}e^{\beta\varepsilon(p)} - 1}p\frac{\partial\varepsilon(p)}{\partial p}p^2dp \\ &= \frac{4\pi g}{3h^3}\int_0^\infty p\frac{\partial\varepsilon(p)}{\partial p}p^2 f(p)dp,\end{aligned} \tag{A.4}$$

where $z = \exp(\frac{\mu}{T})$, $\beta = \frac{1}{T}$ and g is the degeneracy factor. In our case, see Eq. (A.1)

$$\varepsilon(p) = \frac{p^2}{2m} + \frac{1.44 \times 4\pi\hbar^2 q_1 q_2}{Vp^2}, \tag{A.5}$$

and

$$p\frac{\partial\varepsilon(p)}{\partial p} = 2\left[\frac{p^2}{2m} - \frac{1.44 \times 4\pi\hbar^2 q_1 q_2}{Vp^2}\right]. \tag{A.6}$$

Therefore, the pressure is given as

$$\begin{aligned}P &= \frac{4\pi g}{3h^3}\int_0^\infty 2\left[\frac{p^2}{2m} - \frac{1.44 \times 4\pi\hbar^2 q_1 q_2}{Vp^2}\right]p^2 f(p)dp \\ &= \frac{8\pi g}{3h^3}\left\{\frac{1}{2m}\int_0^\infty p^4 f(p)dp \right. \\ &\quad \left. - \frac{1.44 \times 4\pi\hbar^2 q_1 q_2}{V}\int_0^\infty f(p)dp\right\} \\ &= \frac{8\pi g}{3h^3}\left\{\frac{1}{2m}\int_0^\infty p^4 \frac{1}{e^{[\frac{p^2}{2m} + \frac{1.44\times 4\pi\hbar^2 q_1 q_2}{Vp^2} - \mu]/T} - 1}dp \right. \\ &\quad \left. - 2m\frac{A'}{V}\int_0^\infty \frac{1}{e^{[\frac{p^2}{2m} + \frac{1.44\times 4\pi\hbar^2 q_1 q_2}{Vp^2} - \mu]/T} - 1}dp\right\} \\ &= \frac{8\pi g}{3h^3}\left\{\frac{1}{2m}\int_0^\infty p^4 \frac{1}{e^{[\frac{p^2}{2m} + \frac{A'}{V\frac{p^2}{2m}} - \mu]/T} - 1}dp \right. \\ &\quad \left. - 2m\frac{A'}{V}\int_0^\infty \frac{1}{e^{[\frac{p^2}{2m} + \frac{A'}{V\frac{p^2}{2m}} - \mu]/T} - 1}dp\right\},\end{aligned} \tag{A.7}$$

where $A' = \frac{1.44\times 4\pi\hbar^2 q_1 q_2}{2m}$ is introduced. Let us make twice the integral variable transformations,

$$\varepsilon = \frac{p^2}{2m}, \quad p = (2m\varepsilon)^{\frac{1}{2}}, \quad dp = \frac{m}{\sqrt{2m\varepsilon}}d\varepsilon, \tag{A.8}$$

and

$$x = \frac{\varepsilon}{T}, \quad \nu = \frac{\mu}{T}. \tag{A.9}$$

The pressure P of a Bose gas with Coulomb correction becomes

$$\begin{aligned}P &= \frac{8\pi g}{3h^3}\left\{\frac{1}{2m}\frac{(2mT)^{\frac{5}{2}}}{2}\int_0^\infty dx x^{\frac{3}{2}}\frac{1}{e^{x + \frac{A'}{xVT^2} - \nu} - 1} \right. \\ &\quad \left. - 2m\frac{A'}{V}\frac{(2mT)^{\frac{1}{2}}}{2}\int_0^\infty dx x^{-\frac{1}{2}}\frac{1}{e^{x + \frac{A'}{xVT^2} - \nu} - 1}\right\} \\ &= \frac{4\pi g}{3h^3}(2mT)^{\frac{3}{2}}\int_0^\infty dx\left(Tx^{\frac{3}{2}} - \frac{A'}{TVx^{\frac{1}{2}}}\right) \\ &\quad \times \frac{1}{e^{x + \frac{A'}{xVT^2} - \nu} - 1}.\end{aligned} \tag{A.10}$$

Substituting Eq. (A.10) into Eq. (A.3), the free energy density becomes

$$\begin{aligned}\frac{F}{V} &= \rho\mu - \frac{4\pi g}{3h^3}(2mT)^{\frac{3}{2}}\int_0^\infty dx\left(Tx^{\frac{3}{2}} - \frac{A'}{TVx^{\frac{1}{2}}}\right)\frac{1}{e^{x + \frac{A'}{xVT^2} - \nu} - 1} \\ &= \rho T\nu - \frac{4\pi g}{3h^3}(2mT)^{\frac{3}{2}}\int_0^\infty dx\left(Tx^{\frac{3}{2}} - \frac{A'}{TVx^{\frac{1}{2}}}\right) \\ &\quad \times \frac{1}{e^{x + \frac{A'}{xVT^2} - \nu} - 1}.\end{aligned} \tag{A.11}$$

In the limit of no Coulomb correction ($A' = 0$) and $\mu = 0$, $\nu = \frac{\mu}{T} = 0$, the free energy density is given as

$$\begin{aligned}\frac{F}{V} &= -\frac{4\pi g}{3h^3}(2mT)^{\frac{3}{2}}\int_0^\infty dx T x^{\frac{3}{2}}\frac{1}{e^x - 1} \\ &= -0.085g\frac{m^{3/2}T^{5/2}}{\hbar^3},\end{aligned} \tag{A.12}$$

which is the result for an ideal Bose gas at the BEC. When A' is different from zero and $\mu = 0$, Eq. (A.11) can be solved numerically and the results are plotted in Fig. 4 for the d and α BEC.

[1] J. A. Scarpaci *et al.*, Phys. Rev. C **82**, 031301 (2010).
[2] M. Freer and H. Fynbo, Prog. Part. Nucl. Phys. **78**, 1 (2014).
[3] S. Elhatisari *et al.*, Phys. Rev. Lett. **117**, 132501 (2016).
[4] D. J. Dean, Physics **9**, 106 (2016).
[5] S. Kowalski *et al.*, Phys. Rev. C **75**, 014601 (2007).
[6] J. B. Natowitz *et al.*, Phys. Rev. Lett. **104**, 202501 (2010).
[7] R. Wada *et al.*, Phys. Rev. C **85**, 064618 (2012).
[8] L. Qin *et al.*, Phys. Rev. Lett. **108**, 172701 (2012).
[9] G. Röpke *et al.*, Phys. Rev. C **88**, 024609 (2013).
[10] C. Horowitz and A. Schwenk, Nucl. Phys. **A776**, 55 (2006).
[11] S. Typel, H. H. Wolter, G. Röpke, and D. Blaschke, Eur. Phys. J. **A50**, 17 (2014).
[12] P. Danielewicz, R. Lacey, and W. G. Lynch, **298**, 1592 (2002).
[13] J. M. Lattimer and M. Prakash, Science **304**, 536 (2004).
[14] B.-A. Li, L.-W. Chen, and C. M. Ko, Phys. Rep. **464**, 113 (2008).
[15] G. Giuliani, H. Zheng, and A. Bonasera, Prog. Part. Nucl. Phys. **76**, 116 (2014).
[16] H. Zheng and A. Bonasera, Phys. Lett. **B696**, 178 (2011).
[17] H. Zheng and A. Bonasera, Phys. Rev. C **86**, 027602 (2012).
[18] H. Zheng, G. Giuliani, and A. Bonasera, Nucl. Phys. **A892**, 43 (2012).
[19] H. Zheng, G. Giuliani, and A. Bonasera, Phys. Rev. C **88**, 024607 (2013).
[20] H. Zheng, G. Giuliani, and A. Bonasera, J. Phys. G: Nucl. Part. Phys. **41**, 055109 (2014).
[21] S. Wuenschel *et al.*, Nucl. Instrum. Methods A **604**, 578 (2009).
[22] R. Schmitt *et al.*, Nucl. Instr. Meth. A **354**, 487 (1995).
[23] Z. Kohley, Ph.D. thesis, Texas A&M University (2010).
[24] Z. Kohley *et al.*, Phys. Rev. C **83**, 044601 (2011).
[25] Z. Kohley *et al.*, Phys. Rev. C **86**, 044605 (2012).
[26] S. Wuenschel *et al.*, Nucl. Phys. **A843**, 1 (2010).
[27] P. Marini *et al.*, Nucl. Instr. Meth. A **707**, 80 (2013).
[28] S. Wuenschel *et al.*, Phys. Rev. C **79**, 061602 (2009).
[29] A. Bonasera *et al.*, Phys. Rev. Lett. **101**, 122702 (2008).
[30] M. Huang *et al.*, Phys. Rev. C **81**, 044618 (2010).
[31] R. Tripathi *et al.*, Phys. Rev. C **83**, 054609 (2011).
[32] J. Mabiala *et al.*, Phys. Rev. C **87**, 017603 (2013).
[33] S. Typel *et al.*, Phys. Rev. C **81**, 015803 (2010).
[34] M. E. Fisher, Rep. Prog. Phys. **30**, 615 (1967).
[35] R. Minich *et al.*, Phys. Lett. **B118**, 458 (1982).
[36] A. Bonasera *et al.*, La Rivista Del Nuovo Cimento **23**, 1 (2000).
[37] R. Tripathi *et al.*, Int. J. Mod. Phys. E **21**, 1250019 (2012).
[38] K. Huang, *Statistical Mechanics (2nd edition)* (Wiley & Sons, New York, 1987) pp. Chap. 16–17.
[39] K. Hagel *et al.*, Phys. Rev. Lett. **108**, 062702 (2012).
[40] J. Mabiala *et al.*, Phys. Rev. C **90**, 027602 (2014).
[41] P. Marini *et al.*, Phys. Lett. **B756**, 194 (2016).
[42] J. Mabiala *et al.*, Phys. Rev. C **92**, 024605 (2015).
[43] L. D. Landau and E. M. Lifshitz, *Statistical Physics* (Pergamon, New York, 1980).
[44] H. Shen, H. Toki, K. Oyamatsu, and K. Sumiyoshi, .
[45] M. Hempel and J. Schaffner-Bielich, Nucl. Phys. **A837**, 210 (2010).
[46] R. K. Pathria, *Statistical Mechanics (Second Edition)* (Butterworth-Heinemann, 1996).